Chemical composition of tropospheric air masses encountered during high altitude flights (11.5 km) during the 2009 fall Operation Ice Bridge field campaign

Mei Ying Melissa Yang,[1] Stephanie A. Vay,[1] Andreas Stohl,[2] Yonghoon Choi,[1,4] Glenn S. Diskin,[1] Glen W. Sachse,[1,4] and Donald R. Blake[3]

Received 28 March 2012; revised 23 July 2012; accepted 25 July 2012; published 14 September 2012.

[1] As part of the 2009 Operation Ice Bridge campaign, the NASA DC-8 aircraft was used to fill the data-time gap in laser observation of the changes in ice sheets, glaciers and sea ice between ICESat-I (Ice, Cloud, and land Elevation Satellite) and ICESat-II. Complementing the cryospheric instrument payload were four in situ atmospheric sampling instruments integrated onboard to measure trace gas concentrations of CO_2, CO, N_2O, CH_4, water vapor and various VOCs (Volatile Organic Compounds). This paper examines two plumes encountered at high altitude (12 km) during the campaign; one during a southbound transit flight (13°S) and the other at 86°S over Antarctica. The data presented are especially significant as the Southern Hemisphere is heavily under-sampled during the austral spring, with few if any high-resolution airborne observations of atmospheric gases made over Antarctica. Strong enhancements of CO, CH_4, N_2O, $CHCl_3$, OCS, C_2H_6, C_2H_2 and C_3H_8 were observed in the two intercepted air masses that exhibited variations in VOC composition suggesting different sources. The transport model FLEXPART showed that the 13°S plume contained predominately biomass burning emissions originating from Southeast Asia and South Africa, while both anthropogenic and biomass burning emissions were observed at 86°S with South America and South Africa as indicated source regions. The data presented here show evidence that boundary layer pollution is transported from lower latitudes toward the upper troposphere above the South Pole, which may not have been observed in the past.

Citation: Yang, M. Y. M., S. A. Vay, A. Stohl, Y. Choi, G. S. Diskin, G. W. Sachse, and D. R. Blake (2012), Chemical composition of tropospheric air masses encountered during high altitude flights (11.5 km) during the 2009 fall Operation Ice Bridge field campaign, *J. Geophys. Res.*, *117*, D17306, doi:10.1029/2012JD017858.

1. Introduction

[2] While there is a considerable legacy of research on atmospheric composition in the Northern Hemisphere (NH), there is a dearth of information for the Southern Hemisphere (SH), particularly over Antarctica. Interest in the Antarctic atmosphere peaked for a brief period beginning in 1985, when the British Antarctic Survey reported a large unexpected decrease in ozone over the continent [*Jones and Shanklin*, 1995], sparking several airborne campaigns focused on ozone depletion. In 1987, both the NASA ER-2 and DC-8 aircraft supported the Airborne Antarctic Ozone Experiment (AAOE) providing crucial information on how the unique chemistry of the Antarctic atmosphere aided in the destruction of the springtime ozone by chlorofluorocarbons (CFCs) [*Heidt et al.*, 1989]. Seven years later, the NASA ER-2 redeployed for the Airborne Southern Hemisphere Ozone Expedition (ASHOE) to study the chemistry and depletion of ozone over Antarctica and other Southern hemispheric latitudes (NOAA ESRL Chemical Sciences Division, Stratospheric Ozone Layer (Antarctic, Arctic, and Global), 1995, available at http://www.esrl.noaa.gov/csd). Missions subsequent to ASHOE with varying scientific objectives included: APE-GAIA [*Carli et al.*, 1999], ANTCI [*Eisele et al.*, 2008], and AGAMES [*Wada et al.*, 2007; A. Minikin, AGAMES–Antarctic Trace Gas and Aerosol Airborne Measurement Study, 2007, available at http://www.pa.op.dlr.de/aerosol/agames]. In 2009, measurements over Antarctica resumed with the HIAPER Pole-to-Pole Observations (HIPPO) Project focused on the global distribution of carbon dioxide and other trace gases at various latitudes and altitudes over all seasons and multiple years. Measurements over Antarctica, however, comprise a small portion of the HIPPO

[1]Chemistry and Dynamics Branch, NASA Langley Research Center, Hampton, Virginia, USA.
[2]Norwegian Institute for Air Research, Kjeller, Norway.
[3]Department of Chemistry, University of California, Irvine, California, USA.
[4]National Institute of Aerospace, Hampton, Virginia, USA.

Corresponding author: M. Y. M. Yang, Chemistry and Dynamics Branch, NASA Langley Research Center, MS 483, Hampton, VA 23681, USA. (melissa.yang@nasa.gov)

0148-0227/12/2012JD017858

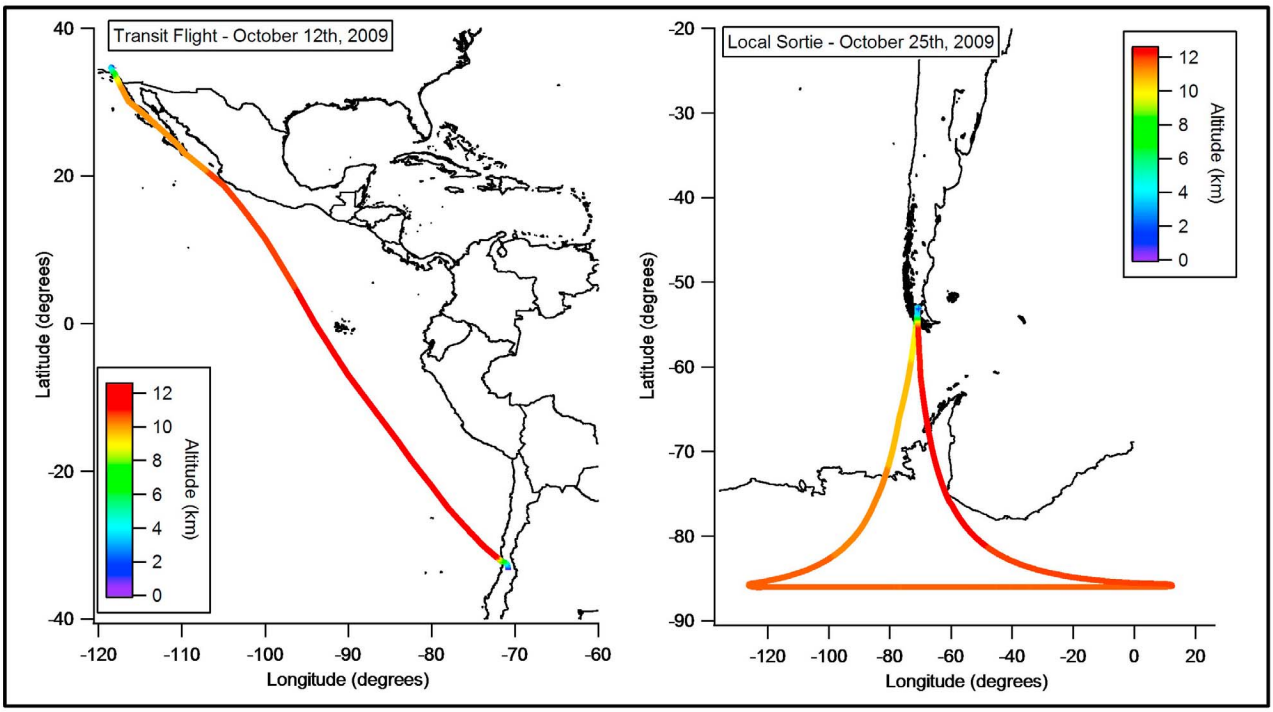

Figure 1. Flight tracks for the 12 October Transit flight from California to Santiago, Chile, and the 25 October local sortie out of Punta Arenas, Chile, down to Antarctica and back.

campaigns and comprehensive flights over the Antarctic continent did not occur (NSF/NCAR, HIAPER Pole-to-Pole Observations, 2011, available at http://hippo.ucar.edu/HIPPO/about-hippo).

[3] In the austral spring of 2009, chemical tracer data acquired during the Operation Ice Bridge (OIB) mission offered a unique glimpse into long-range transport of pollution, penetrating and influencing the composition of the upper troposphere within the SH. This paper examines two pollution events encountered at high altitude (12 km) during the campaign; one at 13°S on the southbound transit, and the other at 86°S. To the best of our knowledge, the observation of distant surface emissions reaching the upper troposphere over the South Polar region has been previously undocumented.

2. Experimental

[4] OIB is a six year NASA airborne campaign that consists of both a NH and SH component. OIB flights are conducted in the Arctic (March–May), and the Antarctic (October–November) of each year to help fill the data-time gap in laser observation of the changes in ice sheets, glaciers and sea ice between the end of ICESat-I (Ice, Cloud, and land Elevation Satellite) in 2009 and the launch of ICESat-II in early 2016 (NASA, ICESat and ICESat-2, 2010, available at http://icesat.gsfc.nasa.gov).

[5] During the 2009 OIB Antarctic deployment, the cryospheric science payload was augmented with four in situ chemical tracer instruments. Three of the instruments made high-resolution (1 Hz) measurements of CO_2, CO, CH_4, N_2O, H_2O, while the fourth collected whole air samples for CFCs, NMHCs, and halocarbons. In situ CO_2 measurements were made using a modified LI-COR model 6252 differential, non-dispersive infrared gas analyzer to achieve both high precision (±0.1 ppmv) and accuracy (±0.25 ppmv) relative to World Meteorological Organization CO_2 primary standards [*Vay et al.*, 2003]. CO, CH_4 and N_2O were measured using a tunable diode laser spectrometer [*Sachse et al.*, 1987] operating in the mid-IR with respective 1σ precisions of 1%, 0.1%, and 0.1%. Water vapor was measured with an open path diode laser hygrometer (DLH) operating in the 1.4 μm spectral region. The precision of the instrument is 1% of the reported mixing ratio [*Diskin et al.*, 2002].

[6] Using the University of California, Irvine (UCI) Whole Air Sampler (WAS), up to 168 samples were collected in 2 L stainless steel canisters each flight. Filled canisters were returned to UCI post-mission and approximately 72 speciated VOCs (C2-C10 hydrocarbons, cycloalkanes, aromatics, monoterpenes, oxygenates, halocarbons, and sulfur compounds) were analyzed from these samples. A complete description of the sample collection and measurement precision, accuracy and detection limit for each VOC is presented in *Simpson et al.* [2010].

[7] OIB consisted of 4 transit and 21 local flights flown out of Punta Arenas, Chile. Chemical tracer data were obtained on the transit flights and 6 of the 21 local sorties. The remaining 15 sorties covered ICESat objectives only. This paper focuses on two flights: the 12 October outbound transit from Palmdale, California, to Santiago, Chile; and a local sortie out of Punta Arenas, Chile, to 86°S on 25 October. The flight tracks for both flights are shown in Figure 1. Complete flight reports can be found on the NASA ESPO website (http://www.espo.nasa.gov/oib/flightDocs.php).

[8] The FLEXPART Lagrangian particle dispersion model [*Stohl et al.*, 2005] was used to characterize the sampled

pollution events. From short segments along the pollution intercepts, 20-day retroplumes were calculated. The model calculations used two different meteorological data sets to verify consistency of the simulated transport: operational analyses from the National Centers for Environmental Prediction's Global Forecast System (GFS) with a resolution of $0.5^\circ \times 0.5^\circ$ and 26 vertical levels and the European Centre for Medium-Range Weather Forecasts' (ECMWF) model with a resolution of $1^\circ \times 1^\circ$ and 91 vertical levels. FLEXPART model output (reported as ns kg^{-1}) is proportional to the residence time of the particles in a given volume of air and corresponds to a potential emission sensitivity (PES). When convolved with the gridded emission fluxes from an emission inventory, maps of potential source contributions (PSC) are obtained. Integrating these maps over the globe, yields a model-calculated mixing ratio contribution of the emitted species at the location of the aircraft measurements. EDGAR fast track 2000 is the source of anthropogenic CO emissions, and biomass burning CO emissions are based on fire locations detected by the MODIS (Moderate Resolution Imaging Spectroradiometer) instrument onboard the Terra and Aqua satellites and a land cover classification [*Stohl et al.*, 2007a]. A full description of the methods used here is given in *Stohl et al.* [2007a].

3. Results and Discussions

[9] The time series of various gas species measured during the two flights are illustrated in Figures 2a and 2b, with the respective plumes demarcated by dashed lines. The high altitude plumes are characterized by enhancements of CO, CH_4 and other tracers over background levels. C_2H_2 is a good tracer for incomplete combustion while C_2Cl_4, a relatively long-lived industrial solvent (2–3 months), is invoked as an industrial tracer [*Simpson et al.*, 2010]. Mean background mixing ratios for each species were determined for the flights, taking the average of the measurements an hour before and after the plume, at similar altitude, location and time. Local background averages were compared to the VOC mixing ratios observed within the plume. The expected enhancements observed during both ascents and descents from/to the airport were attributed to city emissions, however, the enhancements (plumes) observed during flight were not anticipated.

[10] In some cases, absolute values of mixing ratios may be misleading; therefore calculated relative mean enhancements for each trace gas in the two plumes are shown in Figure 3. The degree of mean VOC enhancement within a plume is the relative enhancement of each VOC: ((observed [VOC mixing ratio] – measured [VOC background]) / measured [VOC background]). For example, C_2Cl_4 in plume 1 (Figure 2a) appears significantly more enhanced than that in plume 2 (Figure 2b). However, Figure 3 shows that the enhancement relative to background for plume 2 is slightly greater than that for plume 1; this is largely due to the fact that the average C_2Cl_4 background in plume 2 is lower than that in plume 1.

3.1. Plume 1: Transit Flight From Palmdale, California, to Santiago, Chile

[11] Shortly after takeoff from Palmdale, CA, CO, C_2H_2, and C_2Cl_4 mixing ratios were 95 ppbv, 161 pptv, and 3.5 pptv respectively (10.5 km, 34°N, −117°W), all tracers sharply decreasing as the DC-8 progressed South (Figure 2a). At −13°S, 274°W mixing ratios (CO = 112 ppbv, C_2H_2 = 145 pptv, C_2Cl_4 = 5.8 pptv) comparable to those registered in the NH and significantly enhanced above SH levels were observed at 11 km (Figure 2a). Similar distinct pollution plumes were observed in the PEM-Tropics-A field campaign in September/October 1996 with CO > 100 ppb in the middle-topical troposphere (8–12 km) of the remote South Pacific (10–30°S) [*Singh et al.*, 2000]. Besides the observed enhancements, depletion of several gases is observed in plume 1 (Figure 3). These include CH_3I, CH_2Br_2, $CHBr_3$, $MeONO_2$, $EtONO_2$, 3-$PeONO_2$, 2-$PeONO_2$. Upon further investigation, the same depletion was observed right after take-off from Palmdale, CA. This suggests that interhemispheric transport of NH air down to the SH has occurred, influencing the composition of the plume. Additional analysis will be needed to confirm this hypothesis.

[12] Out of the 72 VOCs measured, plume 1 showed enhancement over background with several biomass burning tracers, CH_4, CO, OCS, CH_2Cl_2, CH_3Cl, CH_3Br, CH_3I, 1,2-DCE, i-$PrONO_2$, 2-$BuONO_2$, C_2H_6, C_2H_2, and C_6H_6 [*Simpson et al.*, 2010]. In plume 1, smaller enhancements in anthropogenic emissions (C_2Cl_4, C_3H_8) were observed in comparison to biomass burning emissions (1,2-DCE, C_2H_2 and C_6H_6), indicating that based on the trace gas data alone, the major contributor was from biomass burning sources. Figure 4 shows the result of the Lagrangian particle dispersion model FLEXPART for a transport time of 20 days. Here we use FLEXPART to characterize the plumes encountered on both flights and the transport of pollution within them from the ground-based source locales to the upper troposphere [*Stohl and Sodemann*, 2010]. FLEXPART was chosen for this analysis as it has been used extensively in other field campaigns (such as GRACE – Greenland Aerosol and Chemistry Experiment) to study aircraft measurements made in the troposphere and lower stratosphere in the summertime Arctic [*Roiger et al.*, 2011]. Illustrated is the column-integrated potential emission sensitivity (PES) which plots the geographical path in which the sampled air mass traveled over time to the point where the DC-8 intercepted the plume at 11 km over the Pacific Ocean west of Lima, Peru. The black dots represent fires active when the air mass passed over them. These detections were based on the MODIS collection 4 data and MOD14 and MYD14 algorithms [*Stohl et al.*, 2007b]. Figure 4 indicates that the main source of the enhanced trace gases observed is from biomass burning in Southeast Asia and South Eastern Africa. Contributions of biomass burning CO from both Southeast Asia and South Eastern Africa accounts for a total simulated biomass burning CO mixing ratio of 15 ppb (not shown). The fires depicted in Figure 4 are attributable to the dry season which occurs from June to October every year in Southeast Asia, with emissions largely from forest fires in Indonesia which have increased since 1980 [*Herawati et al.*, 2006]. The fires shown in Zambia, Mozambique and Madagascar are consistent with the seasonal fire patterns of that time of year; a consequence of the combination of natural burning of seasonally dry grasslands and savannas, as well as man-made activities such as slash and burn agriculture (B. Zimmerman, Mapping Africa's Bush Fires, 2009, available at http://www.27months.com/2009/09/mapping-africa-bush-fires). Pyrogenic emissions are lofted into the upper troposphere and transported across the ocean to

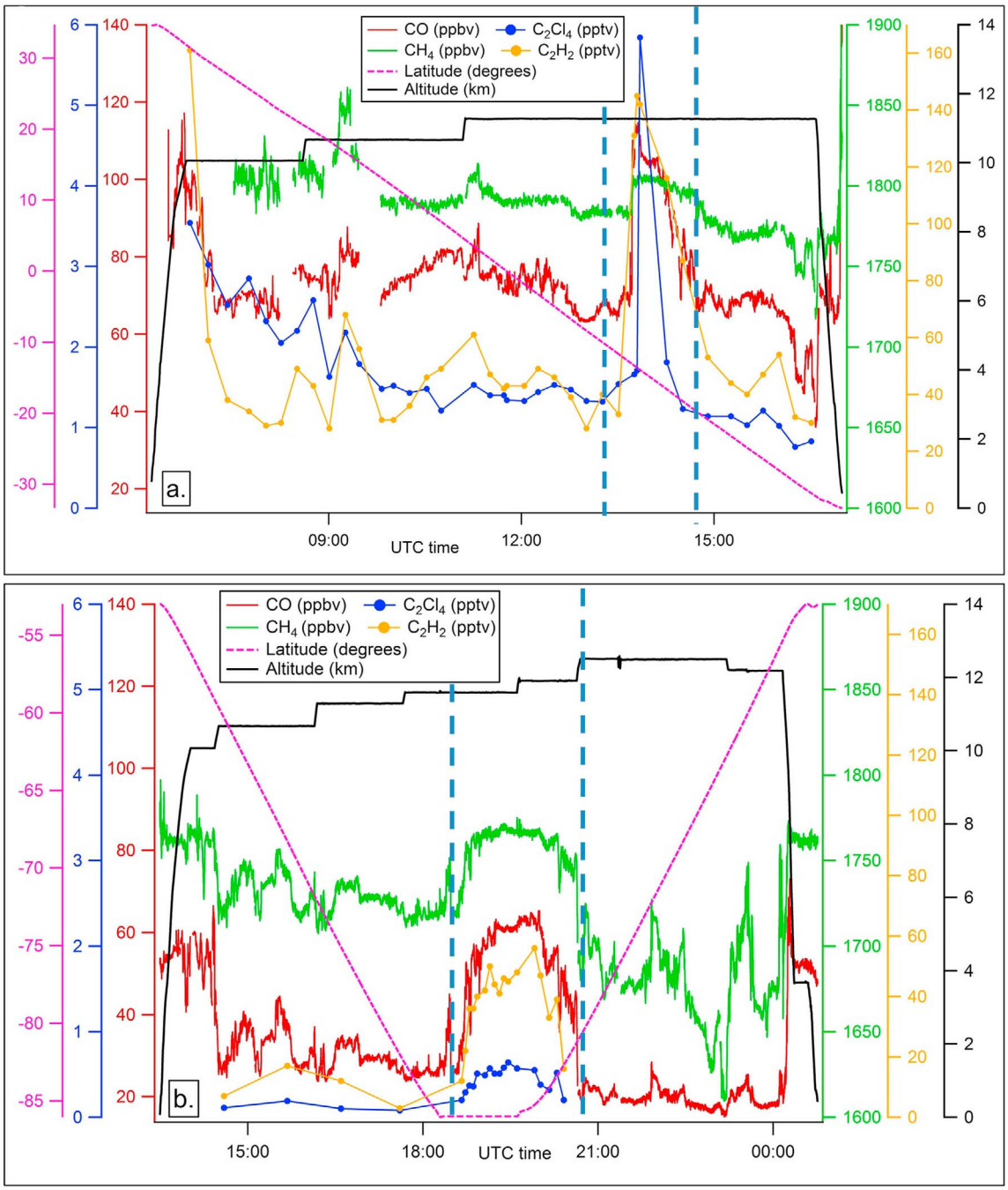

Figure 2. Time series of CO, CH_4, C_2Cl_4, and C_2H_2 during the (a) transit flight on 12 October 2009 over the South Pacific Ocean and (b) the local flight out of Punta Arenas, Chile, to 86°S on 25 October 2009.

the South American coastline as part of the Southern hemispheric circulation pattern.

[13] FLEXPART also produces an anthropogenic CO potential source contribution (PSC) map which highlights the contribution of emissions of only anthropogenic origin (not shown), which yield an additional 5 ppb of CO. Based on the VOC data from the flight, small enhancements of anthropogenic tracers (C_3H_8 and C_2Cl_4) are observed. The anthropogenic CO PSC map plots the distribution of anthropogenic sources contributing to the enhanced tracer emissions observed in the plume at the receptor site. Based on the model results, most of the anthropogenic emissions observed are from Southeast Asia (5 ppbv). When compared to the modeled biomass burning emissions (15 ppbv), this contribution of anthropogenic emissions is small, at the same time it is known that the EDGAR emission inventory used underestimates the emissions in Southeast Asia by probably a factor of two or more [*Forster et al.*, 2004, *Pétron et al.*, 2002]. Furthermore, based on the trace gas data observed in the plume and right after take-off from Palmdale, CA, it is evident that there is NH influence within the plume, which is not shown in the model results. As the FLEXPART

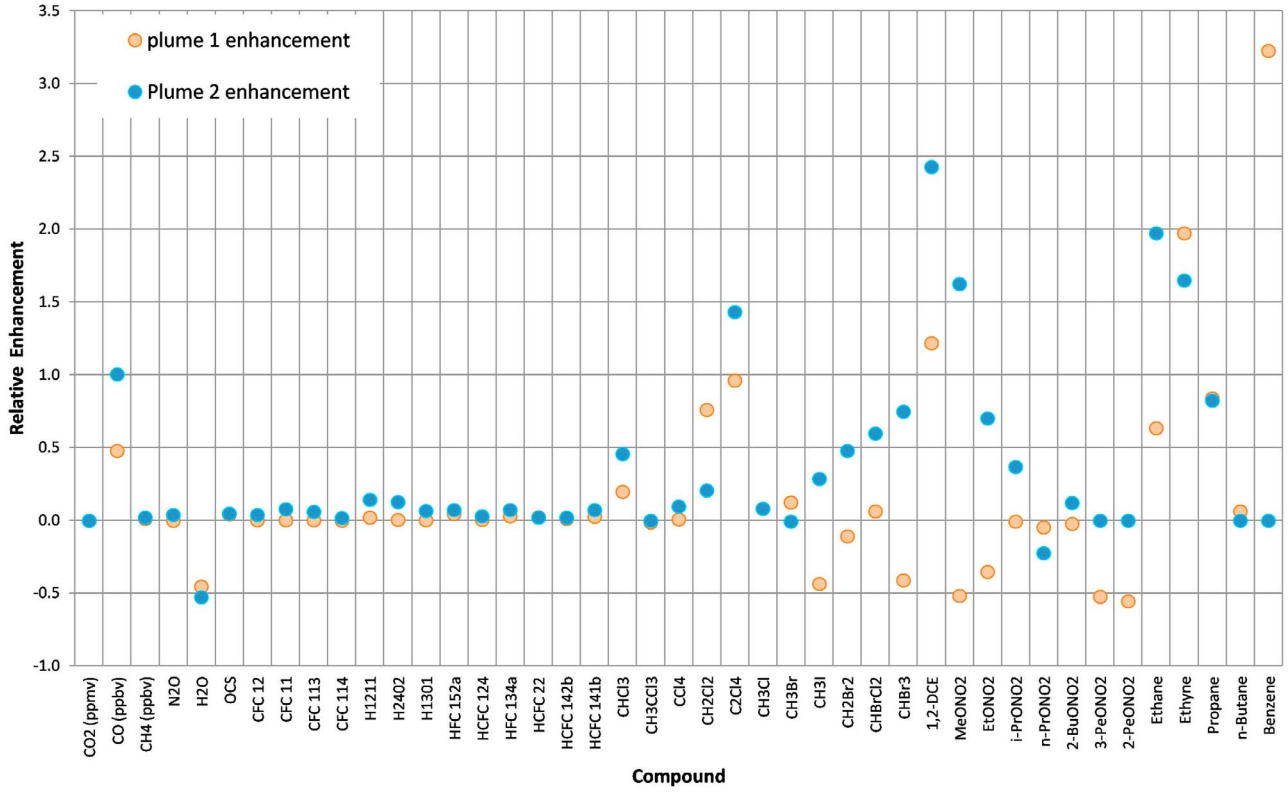

Figure 3. Relative mean enhancements and depletions for the speciated compounds measured in plume 1 (during the transit) and plume 2 (during local 6).

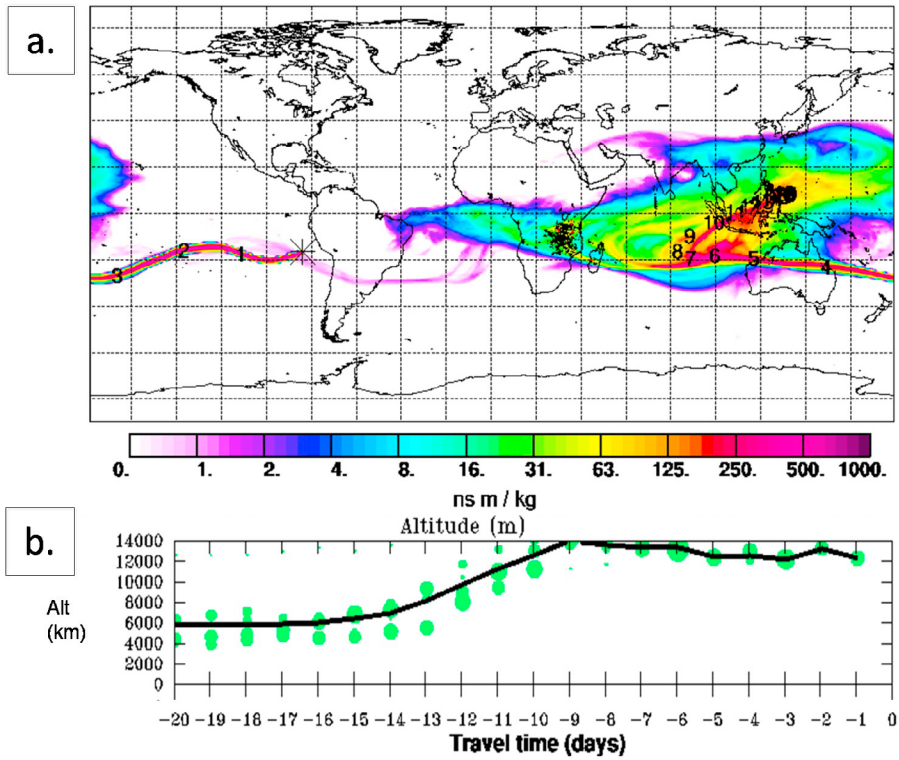

Figure 4. (a, b) FLEXPART modeled data for plume 1 intercepted on 12 October 2009.

Table 1. Enhancement Ratios and Correlation Coefficients Calculated for Several Trace Gases Measured Within Both Plume 1 and Plume 2

Species	Plume 1 Slope (pptv/ppbv CO)	R^2	Plume 2 Slope (pptv/ppbv CO)	R^2
CO_2	0.0017 ± 0.0014 (ppm/ppb)	0.55	1.9 ± 0.88 (ppm/ppb)	0.38
CH_4	0.26 ± 0.065 (ppb/ppb)	0.91	0.71 ± 0.13 (ppb/ppb)	0.83
N_2O	−6.7 ± 3.8e + 006 (ppb/ppb)	0.181	0.24 ± 0.026 (ppb/ppb)	0.94
OCS	1.9 ± 0.92	0.71	35 ± 93	0.11
$CHCl_3$	0.031 ± 0.012	0.84		
CH_2Cl_2	0.15 ± 0.067	0.79		
CH_3Br	0.044 ± 0.016	0.85		
CH_3I	0.00035 ± 0.00013	0.85		
CH_3Cl	4.9 ± 5.2	0.43	5.8 ± 2.6	0.53
$CHBr_3$	0.0027 ± 0.00030	0.98		
C_2Cl_4	0.077 ± 0.080	0.48	0.016 ± 0.0066	0.60
1,2 DCE	0.13 ± 0.035	0.90	0.18 ± 0.070	0.61
i-$PrONO_2$	0.015 ± 0.0043	0.89		
2-$BuONO_2$	0.0053 ± 0.0017	0.87		
C_2H_2	2.0 ± 0.066	0.99	1.9 ± 0.35	0.85
C_2H_6	5.1 ± 0.22	0.99	8.9 ± 1.4	0.89
C_3H_8	1.3 ± 0.061	0.99	0.82 ± 0.28	0.53
C_6H_6	0.55 ± 0.067	0.98		

backward calculations do not extend back further than 20 days, it can only be used to study recent history of the air mass. It is likely that the NH influence extends backward in time for more than 20 days, and thus cannot be fully captured by the presented simulations, but can be seen in the measured signatures of the longer-lived tracers. Other discrepancies observed between the observed CO enhancements and the total simulated CO enhancement (which is considerably smaller than), is most likely attributable to the large uncertainties of the biomass burning emissions as well as the advection of higher background CO from the NH.

[14] Enhancement ratios and correlation coefficients (R^2) were calculated for each chemical tracer relative to CO within both plumes using Orthogonal Distance Regression (ODR) (Table 1). We note that compounds emitted from both anthropogenic and biomass burning sources can undergo chemical reactions in the atmosphere that may either enhance or deplete their mixing ratios during transport. This is essentially dependent on the season, latitude and the compounds' individual atmospheric lifetimes and can affect the calculated enhancement ratio of a trace gas species. However, while the chemical composition of the plume may change over time during transport from the emission source, it is the composition of the plume at the receptor site that ultimately affects the local atmosphere.

[15] Based on the calculated enhancement ratios, the tracers enhanced in plume 1 (CH_4, $CHCl_3$, CH_2Cl_2, CH_3Br, $CHBr_3$, 1,2 DCE, C_2H_4, C_2H_2, C_3H_8 and C_6H_6) (Figure 3) show excellent correlation with CO ($R^2 > 0.75$) (Table 1). Most are biomass burning indicators except for C_3H_8, $CHCl_3$ and $CHBr_3$. C_2Cl_4 though showing significant enhancement with CO has a weaker correlation ($R^2 = 0.48$). All four anthropogenic tracers, highlighted here have different photochemical lifetimes: C_3H_8 (11 days), $CHCl_3$ (3–5 months), $CHBr_3$ (11 months) and C_2Cl_4 (2–3 months) [*Simpson et al.*, 2011] which serve mainly as a reference as they were calculated based on conditions found in the summer, high northern latitudes and will likely be slightly different for the austral spring. Based on the anthropogenic CO PSC map (not shown), the source of these trace species are from Indonesia. From the photochemical lifetimes of the enhanced trace gases we estimate the age of the plume to be at least 9 days old.

3.2. Plume 2: OIB Local Flight 6: Round Trip High-Altitude Flight (>10.5 km) From Punta Arenas, Chile, to Antarctica (86°S)

[16] Few in situ trace gas measurements have been made at high altitude (>10.5 km) over the South Pole [*Romashkin et al.*, 2001]. *Stohl and Sodemann* [2010] state that direct transport of material from other continents to Antarctica does not typically occur due to its remote location. Based on their model calculations, air at 5–8 km above the Antarctic Plateau has an almost exclusively stratospheric origin, even though this is least pronounced in late winter/early spring. However, our data collected at 86°S indicate a pronounced tropospheric influence at an altitude of 11.5 km, which is 2.0 km above the climatologically mean tropopause [*Zängl and Hoinka*, 2001], where such an observation is somewhat unexpected. Retroplume plots as well as daily weather maps were used to track the observed air mass before it was sampled. Prior to intersection with the DC-8 aircraft, the air mass traveled mainly in the lower troposphere over the South Atlantic Ocean, which was then subsequently lifted into the stratosphere by the warm conveyor belt of a cyclone near 30°E just off the shore of the Antarctic continent 7–10 days prior. The air circled in an anti-cyclone and left the anti-cyclone only about one day before the measurement was taken. Since ozone was not measured during OIB, we use N_2O and CFC-12 as stratospheric tracers [*Nevison et al.*, 2007]. Figure 5 shows the relationship observed between N_2O and CFC-12 during the entire flight. The enhancement in both tracers show evidence that the plume encountered is of tropospheric origin (blue oval in Figure 5). Similar enhancement in both CFC-12 and N_2O is observed in plume 1.

[17] The time series shown in Figure 2b reveals enhancement of both anthropogenic and biomass burning trace gases for this flight. Similar to the transit flight, the plume was identified by enhancement of CO and most other tracers. Although the enhancements observed in plume 2 for most trace gases are smaller than those observed in plume 1, they are notable given the remoteness of the location. From Table 1, CO_2, CH_4, N_2O, OCS, CH_3Cl and C_2H_6 show greater enhancement, however only CH_4, N_2O and C_2H_6 are tightly correlated with CO ($R^2 > 0.75$). Enhancements were also observed in the anthropogenic tracer, C_3H_8. Under further investigation into the possible sources of the plume, the CO-CH_4 relationships reveal the presence of an air mass with multiple source regions (Figure 6a). Superimposed onto the CO-CH_4 plot (Figure 6b) is the scaled WAS C_2Cl_4 data. The WAS data points shown in the graph indicate that the possible main source of the air mass is anthropogenic, with little to no biomass burning influence.

[18] FLEXPART retroplumes were calculated for plume 2, encountered on 25 October 2009. Although the emission influence from the past 20 days is generally small for the plume, enhancements clearly show both biomass burning and anthropogenic influence. Figure 7 shows the result of

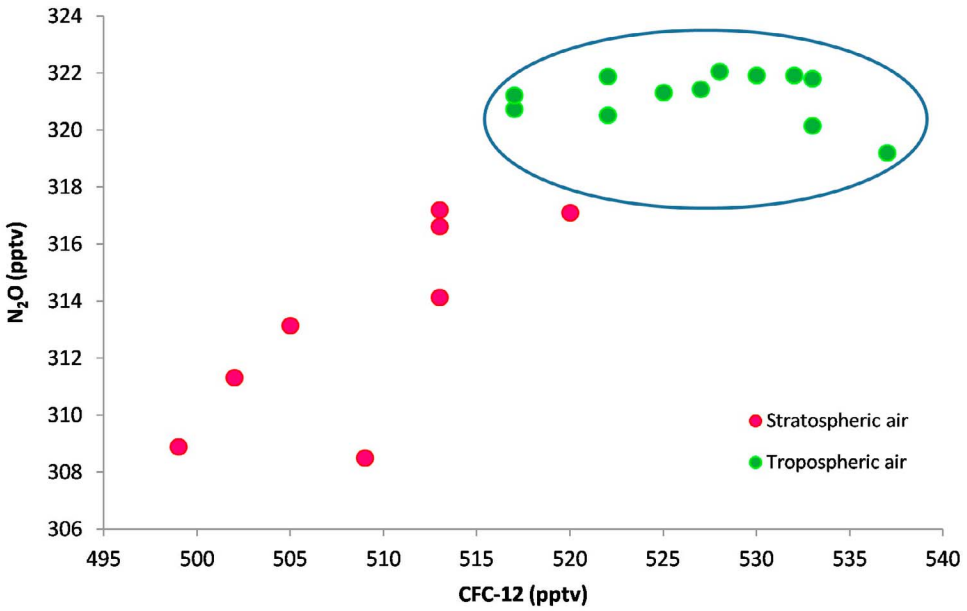

Figure 5. N_2O and CFC-12 from WAS during the 25 October flight.

the FLEXPART model for a transport time of 20 days and contains five common modeled data product plots. The column-integrated PES plot (Figure 7a) highlights the geographical path in which the observed air mass traveled over time to the point where the DC-8 intercepted the plume at 11.5 km over Antarctica, while Figure 7c plots the modeled back trajectory altitude of plume 2 during its transport 20 days prior to intersection with the DC-8. The black dots in Figure 7a highlight the fires actively burning when the air mass passed over them. Figure 7a clearly shows that the main source of the enhanced biomass burning tracers observed is from Southernmost Africa and South America. While the total contribution is small, one would also expect enhanced CO background from emissions older than the 20 days of the backward calculation for a midlatitude tropospheric air mass compared to a stratospherically influenced one. These biomass burning source regions are different from those determined for plume 1. Both Southern Africa and South America have their dry seasons from May to October each year, which is when most of the fires typically occur. In South America, most of the fires occur in grassland and savanna environments, both due to man and natural causes. However, in Angola, South Africa, similar to that in Zambia, Mozambique and Madagascar above, the trees and grass are mostly of the savanna biome which becomes extremely flammable during the dry season. In Southern Africa, 90% of all fires are man-made, purposely set in order to clear land for agricultural use (L. Krock, The World on Fire, NOVA online, 2002, available at http://www.pbs.org/wgbh/nova/fire/world.html#top). The total contribution of emissions of only biomass burning origin from South America and South Africa combined is 2.5 ppbv (not shown).

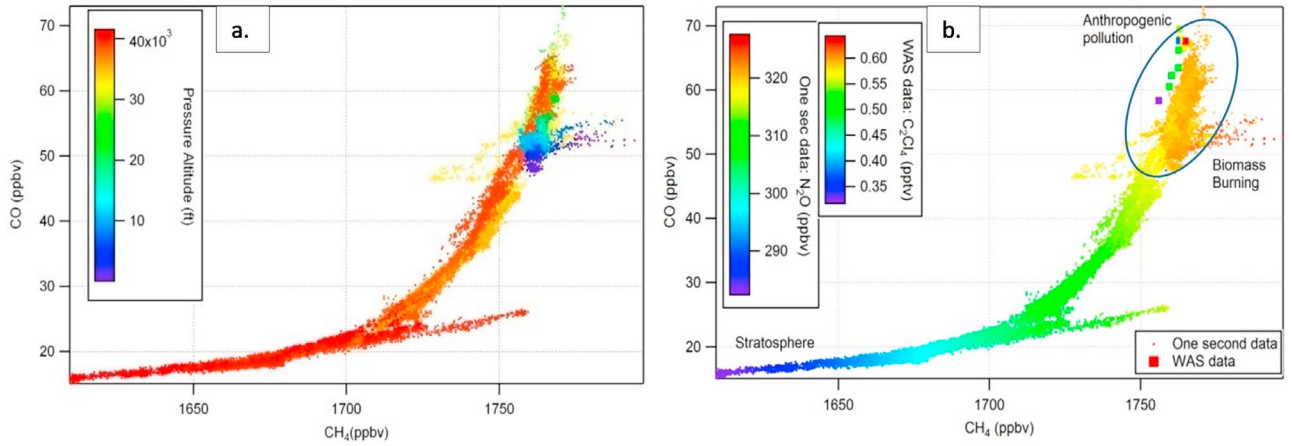

Figure 6. (a, b) CO-CH_4 relationships plotted for the entire local 6 flight, highlighting the presence of at least two different sources of trace gas emissions observed in plume 2.

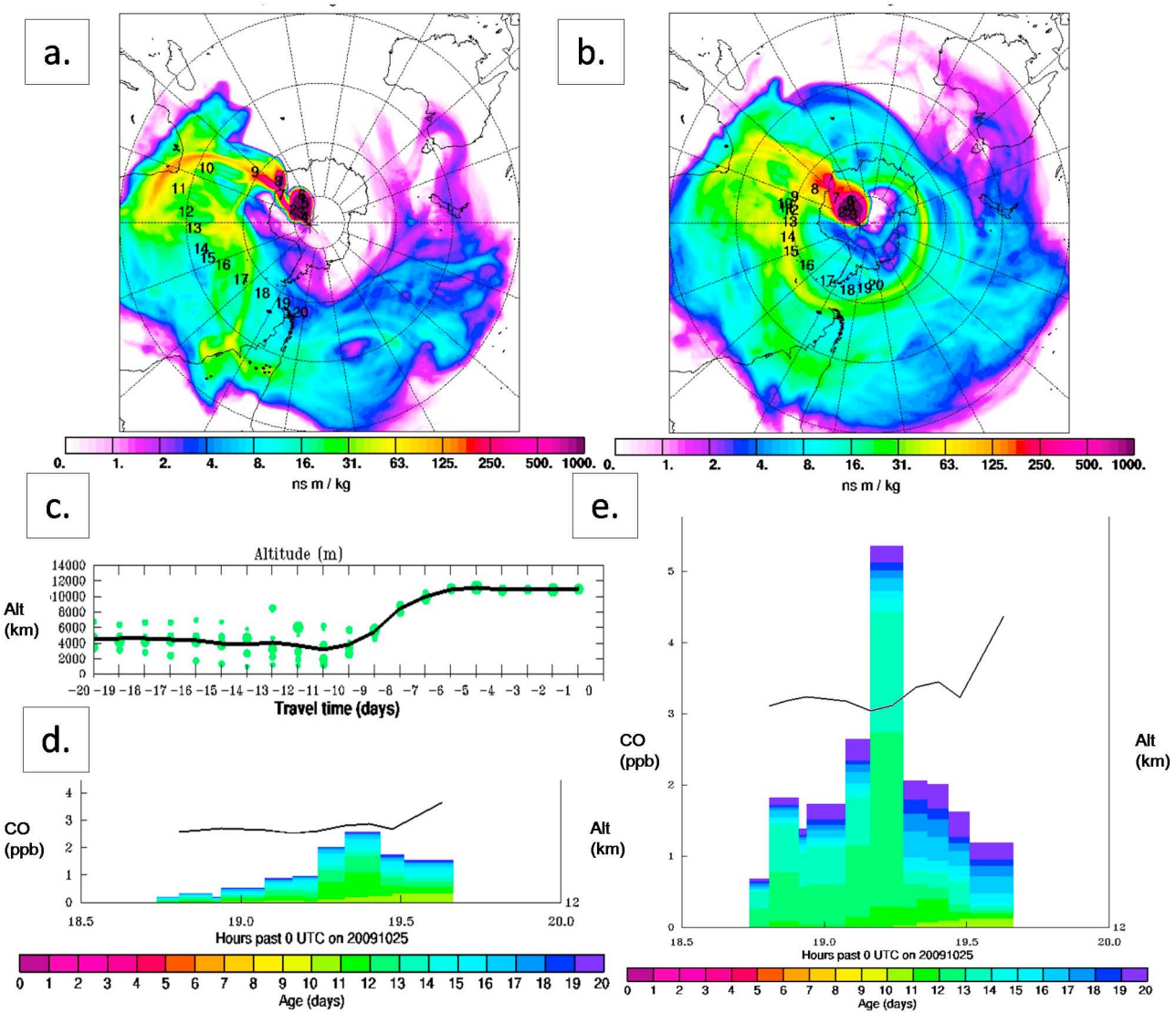

Figure 7. (a–e) FLEXPART modeled data for plume 2 intercepted on 25 October 2009.

[19] Using the FLEXPART model, we also looked at the anthropogenic CO PSC map (not shown), with anthropogenic CO contribution totaling 2.6 ppbv; 2.3 ppbv from Africa, and 0.3 ppbv from South America. For plume 2, both the anthropogenic and biomass burning emission contributions to the plume are approximately equal.

[20] It is important to note that limitations of the model may also arise with the accuracy of the meteorological input data as well as the limited experience in terms of the accuracy of the transport model calculations specifically over the Antarctic lower stratosphere. However, these limitations have been countered to the best of our capabilities by using input data from two meteorological centers (ECMWF and GFS). The results between the models are consistent, with the source regions of the plume indicated by the two simulations being the same, adding additional confidence to our simulations. This confidence level is highlighted in the similarity in results in Figures 7a (ECMWF input) and 7b (GFS input). In an ECMWF newsletter, it is stated that current ECMWF forecasts for both Hemispheres are of similar accuracy (European Centre for Medium-Range Weather Forecasts, ECMWF Background and History, 2011, available at http://www.ecmwf.int/about/corporate_brochure/leaflets/Background-History-2012.pdf).

[21] The FLEXPART modeled results, also allow us to determine the approximate age of the plume. Figures 7d and 7e are spatial integration of the PSC map (shown in Figure 7a) which yield a calculated mixing ratio at the receptor. Based on the known timing of the PSCs, the mixing ratios are displayed in the plots as a function of time elapsed since the emission occurred [*Stohl et al.*, 2007b]. Figures 7d and 7e are age plots for both anthropogenic and biomass burning emissions CO respectively. Based on both plots, the respective ages of emissions found within plume 2 are greater than 9 days (shown previously in the observed trace gas measurement of C_2H_6: τ = 9 days) and extend to the maximum modeled time of 20 days backward, making additional contributions from even more aged emissions likely. The paucity of data available at this high altitude and

remote location preclude us from comparing our results to previous findings.

4. Conclusions

[22] During the 2009 fall OIB campaign, pollution plumes were encountered at high altitude during a transit flight from Palmdale, California, to Santiago, Chile (12 October 2009), and a local sortie from Punta Arenas, Chile, to Antarctica (25 October 2009). Examination of the chemical tracer data in concert with the FLEXPART model indicate different source regions for the pollution. Trace gas data obtained during the transit flight (plume 1) shows a greater contribution from biomass burning than anthropogenic emissions. This is reinforced with the FLEXPART modeled data where plume 1 is dominated by biomass burning emissions from Southeast Asia and South Eastern Africa (15.1 ppbv), with some anthropogenic contribution coming from Southeast Asia (4.7 ppbv). There is also evidence of NH influence in plume 1 based on observed enhancements and depletions of several trace gases such as C_2H_2 and CH_3I respectively. For the plume intercepted over Antarctica (plume 2), the observed trace gas measurements suggest that the main source of emissions are of anthropogenic origin (C_3H_8, C_2Cl_4), however the FLEXPART modeled data suggests that the air mass encountered is equally dominated by biomass burning emissions mainly from South Africa (2.5 ppbv) and anthropogenic emissions from both South Africa and South America (2.6 ppbv) . The discrepancy in observed and modeled results could be due to a variety of reasons. The geographical regions mentioned are all affected by the dry season that plays an important role in the extent of fires occurring during this time. Pyrogenic emissions can be injected directly into the atmosphere at higher altitudes and transported over long distances to the receptor point over Antarctica [*Rio et al.*, 2010]. This could be a possible explanation for the presence of biomass burning tracers in the upper troposphere at latitude 86°S. The FLEXPART modeled results also shows some local boundary layer influence in plume 2. Interestingly enough, the FLEXPART model does not take into account any direct lofting mechanism, hence suggesting direct transport of boundary layer pollution up into the upper troposphere. Unfortunately, little to no high altitude data currently exists for trace gas measurements during the austral spring over Antarctica. In order for us to completely understand this phenomenon observed, more airborne in situ measurements are needed over the region. Further understanding into the complex meteorological conditions that currently exist over the South Pole and how this might influence the transport of trace gases from distant and local surface sources up into the upper troposphere/lower stratosphere over Antarctica is essential to accurately characterize the air masses observed and their influence on this remote landmass. The unique chemical reactivity of the Antarctic as a whole warrants a better understanding of the chemistry that is occurring and the impact this might have on the atmosphere.

[23] **Acknowledgments.** Research for the project was funded by NASA's Upper Atmosphere Research Program (UARP). A.S. was supported by the Norwegian Research Council in the framework of the CLIMSLIP project. Special thanks to the OIB Science Team, the DACOM/DLH research group, AVOCET research group, and the UCI Blake research group. Special thanks to the reviewers from *Journal of Geophysical Research* in helping to further refine and improve our paper.

References

Carli, B., U. Cortesi, and G. DeRossi (1999), Airborne Polar Experiment Geophysica Aircraft In Antarctica (APE-GAIA): A remote sensing chemistry mission, paper presented at Fourth International Airborne Remote Sensing Conference and Exhibition, Environ. Res. Inst. of Mich., Ottawa.

Diskin, G. S., J. R. Podolske, G. W. Sachse, and T. A. Slate (2002), Open-path airborne tunable diode laser hygrometer, *Proc. SPIE*, *4817*, 196, doi:10.1117/12.453736.

Eisele, F., et al. (2008), Antarctic Tropospheric Chemistry Investigation (ANTCI) 2003 overview, *Atmos. Environ.*, *42*(12), 2749–2761, doi:10.1016/j.atmosenv.2007.04.013.

Forster, C., et al. (2004), Lagrangian transport model forecasts and a transport climatology for the Intercontinental Transport and Chemical Transformation 2002(ITCT 2k2) measurement campaign, *J. Geophys. Res.*, *109*, D07S92, doi:10.1029/2003JD003589.

Heidt, L. E., J. F. Vedder, W. H. Pollock, R. A. Lueb, and B. E. Henry (1989), Trace Gases in the Antarctic Atmosphere, *J. Geophys. Res.*, *94*(D9), 11,599–11,611, doi:10.1029/JD094iD09p11599.

Herawati, H., H. Santoso, and C. Forner (2006), Forest Fires and climate change in Indonesia: Background document for the Southeast Asia kick-off meeting of the project Tropical Forests and Climate Change Adaptation ("TroFCCA"), report, Cent. for Int. For. Res., Bogor, Indonesia. [Available at http://docs.google.com/viewer?a=v&q=cache:EC6ZE5CWCl0J:www.cifor.cgiar.org/trofcca/asia/docs/Forest%2520Fire%2520%26%2520CC.pdf+indonesian+fire+season&hl=en&gl=us&pid=bl&srcid=ADGEESh9kU4B-l4Vi1fCS7-JttAIIoIfOfqc9nH9NoegVWtnbTsiGLd9K4d_v6s6YWluEa1ft751d-Ki6KzlpiPgYD3qvaJfrgNLiCpBlYEuSvAkkw7_BqAsAi6hApR0mt-QiZk9Wzxsju&sig=AHIEtbQDGIr83lE85WQRf8EsnKf7rZ052Q.]

Jones, A. E., and J. D. Shanklin (1995), Continued decline ozone over Halley, Antarctica, since 1985, *Nature*, *376*, 409–411, doi:10.1038/376409a0.

Nevison, C. D., N. Mahowald, R. Weiss, and R. Prinn (2007), Interannual and seasonal variability in Atmospheric N_2O, *Global Biogeochem. Cycles*, *21*, GB3017, doi:10.1029/2006GB002755.

Pétron, G., C. Granier, B. Khattatov, J.-F. Lamarque, V. Yudin, J.-F. Müller, and J. Gille (2002), Inversion modeling of carbon monoxide surface emissions using Climate Monitoring and Diagnostics Laboratory network observations, *J. Geophys. Res.*, *107*(D24), 4761, doi:10.1029/2001JD001305.

Rio, C., F. Hourdin, and A. Chédin (2010), Numerical simulation of tropospheric injection of biomass burning products by pyro-thermal plumes, *Atmos. Chem. Phys.*, *10*, 3463–3478, doi:10.5194/acp-10-3463-2010.

Roiger, A., et al. (2011), In-situ observation of Asian pollution transported into the Arctic lowermost stratosphere, *Atmos. Chem. Phys.*, *11*, 10,975–10,994, doi:10.5194/acp-11-10975-2011.

Romashkin, P. A., D. F. Hurst, J. W. Elkins, E. G. Dutton, R. E. Dunn, F. Moore, R. C. Myers, and B. D. Hall (2001), In situ measurements of long-lived trace gases in the lower stratosphere by gas chromatography, *J. Atmos. Oceanic Technol.*, *18*(7), 1195–1204, doi:10.1175/1520-0426(2001)018<1195:ISMOLL>2.0.CO;2.

Sachse, G. W., G. F. Hill, L. O. Wade, and M. G. Perry (1987), Fast-response, high-precision carbon monoxide sensor using a tunable diode laser absorption technique, *J. Geophys. Res.*, *92*(D2), 2071–2081, doi:10.1029/JD092iD02p02071.

Simpson, I. J., et al. (2010), Characterization of trace gases measured over Alberta oil sands mining operations: 76 speciated C_2–C_{10} volatile organic compounds (VOCs), CO_2, CH_4, CO, NO, NO_2, NO_y, O_3 and SO_2, *Atmos. Chem. Phys. Discuss.*, *10*, 18,507–18,560, doi:10.5194/acpd-10-18507-2010.

Simpson, I. J., et al. (2011), Boreal forest fire emissions in fresh Canadian smoke plumes: C_1–C_{10} volatile organic compounds (VOCs), CO_2, CO, NO_2, NO, HCN and CH_3CN, *Atmos. Chem. Phys. Discuss.*, *11*, 9515–9566, doi:10.5194/acpd-11-9515-2011.

Singh, H. B., et al. (2000), Biomass burning influences on the composition of the remote South Pacific troposphere: Analysis based on observations from PEM-Tropics-A, *Atmos. Environ.*, *34*(4), 635–644, doi:10.1016/S1352-2310(99)00380-5.

Stohl, A., and H. Sodemann (2010), Characteristics of atmospheric transport into the Antarctic troposphere, *J. Geophys. Res.*, *115*, D02305, doi:10.1029/2009JD012536.

Stohl, A., C. Forster, A. Frank, P. Seibert, and G. Wotawa (2005), Technical note: The Lagrangian particle dispersion model FLEXPART version 6.2, *Atmos. Chem. Phys.*, *5*, 2461–2474, doi:10.5194/acp-5-2461-2005.

Stohl, A., et al. (2007a), Arctic smoke: Record high air pollution levels in the European Arctic due to agricultural fires in Eastern Europe in spring 2006, *Atmos. Chem. Phys.*, *7*, 511–534, doi:10.5194/acp-7-511-2007.

Stohl, A., J. F. Burkhart, S. Eckhardt, D. Hirdman, and H. Sodemann (2007b), An integrated internet-based system for analyzing the influence of emission sources and atmospheric transport on measured concentrations of trace gases and aerosols, report, Norwegian Inst. for Air Res., Kjeller, Norway. [Available at http://zardoz.nilu.no/~andreas/publications/web_based_tool.pdf.]

Vay, S. A., et al. (2003), Influence of regional-scale anthropogenic emissions on CO_2 distributions over the western North Pacific, *J. Geophys. Res.*, *108*(D20), 8801, doi:10.1029/2002JD003094.

Wada, M., T. Yamanouchi, and A. Herber (2007), Airborne atmospheric observations in the Antarctic under NIPR-AWI cooperation (ANTSYO-II/AGAMES), in *International symposium: Asian collaboration in IPY 2007–2008, Tokyo, Japan, March 1, 2007, Japan International Polar Year National Committee*, pp. 218–221, Tokyo, Jpn. IPY Natl. Comm., Tokyo.

Zängl, G., and K. P. Hoinka (2001), The tropopause in the polar regions, *J. Clim.*, *14*, 3117–3139, doi:10.1175/1520-0442(2001)014<3117:TTITPR>2.0.CO;2.